# Estimation of spatial and temporal water requirements of grain amaranth using satellite, local and virtual weather stations datasets in Uganda

Joseph Kyagulanyi[1], Isa Kabenge[1], Noble Banadda[1], John Muyonga[2],
Peter Mulamba[1], Nicholas Kiggundu[1*]

(1. *Department of Agricultural and Biosystems Engineering, Makerere University, P.O. Box 7062, Kampala, Uganda*;
2. *Department of Food Technology and Nutrition, Makerere University P.O Box 7062 Kampala, Uganda*)

**Abstract:** In this study, an integrated approach incorporating Remote Sensing (RS), Geographical Information System (GIS), local meteorological weather stations' data and NASA's virtual meteorological stations' data were used to quantify Grain Amaranth (GA) water requirements in Uganda. Penman-Monieth method within CropWAT8 model and Surface Energy Balance Algorithm for Land (SEBAL) Model was used to quantify the evapotranspiration. Normalized Difference Vegetation Index (NDVI), daily spatial distribution of Evapotranspiration (ET), Land Surface Temperature (LST) and surface albedo were extracted from satellite imagery. The ratio of effective rainfall (Pe) to Potential Evapotranspiration (PET) – (Pe/PET) and time series for NDVI were computed to determine the growth stage of GA in different areas. The GA water demand was the highest in Karamoja sub-region (467.5 mm/season) and the lowest in Tororo (174.1 mm/season). The growing season for GA in most areas of Uganda was from March to December. Estimation of evapotranspiration in Karamoja sub-region with SEBAL model corresponded to the NDVI extracted, especially for highly vegetated areas. CROPWAT indicated that if GA was planted during the late September and early October in Karamoja sub-region, despite the decreasing moisture levels, the crop could have sufficient water supply during emergence to maturity. The ability to utilize low available moisture levels makes GA a potential crop to bridge the gap (due to the elongated drought) for the food production cycle in Karamoja sub-region.
**Keywords:** grain amaranth, water requirement, remote sensing, SEBAL, evapotranspiration, Uganda
**DOI:** 10.3965/j.ijabe.20160902.1676

## 1　Introduction

Uganda's agriculture is mostly rainfed making it

vulnerable to the effects of prolonged droughts. The semi-arid areas of the country which experience chronic water stress stretch from southwest through central to northeast. The chronic water stresses and prolonged droughts significantly increase the levels of food insecurity, increase food prices and have general negative effects on the economy. Although other areas also grapple with the prolonged chronic droughts, Karamoja sub-region in the northeastern part of country is most affected. Temperatures in Karamoja sub-region are high, with an average daily maximum range of 28$^{\circ}$C to 32.5$^{\circ}$C to a daily average minimum of between 15$^{\circ}$C to 18$^{\circ}$C. The relative humidity in the sub-region is low usually less than 40%. These conditions result in high atmospheric demand, vapour pressure deficit and corresponding elevated ET[1]. The soils in Karamoja sub-region are

largely black to dark grey clays with low organic matter as compared to loams found in other fertile parts of Uganda. These soils have a medium storage capacity and may be productive when irrigated[2]. To safeguard the continuity of food production in Karamoja sub-region, viability of an early maturing, drought tolerant and infertile soil tolerant crop Grain Amaranth (GA) was studied. GA matures within 60 to 90 days as compared to maize, millet and sorghum whose maturity period is between 115 to 120 days[3]. According to Muyonga et al.[4], GA can provide both the nutritional and food security benefits, and an extra income to improve livelihoods in drought prone areas of Uganda. Although GA has these opportunities and benefits, the production and consumption of this crop in Uganda is still limited. Introduction of GA in Karamoja sub-region and other climatic zones in Uganda requires knowledge about the spatial and temporal variability of evapotranspiration (ET), crop water demands and soil suitability. Due to inaccuracy, imprecision, uncertainty of weather variables used to compute ET in addition to low coverage of weather stations in Uganda, Remote Sensing (RS), Geographical Information System (GIS), openly available virtual meteorological whether data was used to provide reliable measures of ET. Application of RS and GIS to estimate ET and mapping of soils properties has been demonstrated[5,6]. Surface Energy balances Algorithm for Land (SEBAL) can be adopted to quantify the evapotranspiration at regional scale. SEBAL computes the surface energy balance based on an instantaneous time scale for each pixel of a satellite image[7,8]. The model has been applied in different basins of the world, including Snake River Basin in Idaho, USA[9], the Lake Naivasha drainage basin in Kenya[10], all River Basins in Sri Lanka[11] and the Indus Basin in Pakistan[12]. The accuracy of SEBAL in computing ET is 85% on daily basis and 95% on a seasonal basis[13]. In this study, an integrated approach incorporating Remote Sensing (RS), Geographical Information System (GIS), local meteorological weather stations' data and NASA's virtual meteorological stations' data was used to quantify GA water requirements for different climatic zones of Uganda. The potential for GA to bridge the gap in the food

production cycle due to the elongated drought in Karamoja sub-region was investigated.

## 2   Materials and methods

### 2.1   Description of the study area

Uganda, a landlocked country, is found within the East African plateau lying mostly between latitudes $4^oN$ and $2^oS$ and longitudes $29^oW$ and $35^oE$ (Figure 1). Uganda covers an area of 241 551 km$^2$ of which open water and swamps cover 41 743 km$^2$, Land area is 199 807 km$^2$ (Uganda Bureau of Statistics[14]). Uganda's climate is tropical, with rainy seasons occurring during the months of March to May and September to November, while the months December to February, and it from June to August comprises of Uganda's two dry seasons. Apart from rainfall, other weather variables including temperature, humidity and evaporation are consistent throughout the year.
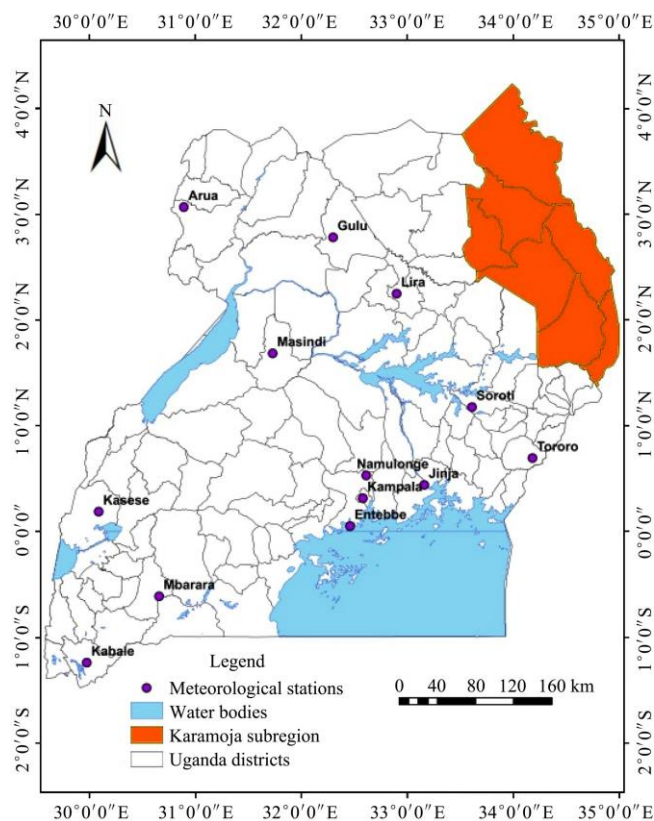


Figure 1    Location of Karamoja sub-region meteorological
stations

Karamoja sub-region (Figure 1) located in northeastern part of the country receives about 760 mm to 1000 mm of rainfall with a dry season of four months which is longer than the average length of dry season (less than three months) in Uganda. The length of the

dry season introduces a break in the food production cycle of the sub-region. Often supplementary irrigation is required to enable crops with longer growth periods to complete their growth cycle. Over 80% of the region is flat to gently sloping land with average slope of 3.41%.

## 2.2 Data collection

Average monthly maximum and minimum temperature, rainfall, relative humidity for 14 stations for the years from 2000 to 2011 was obtained from the Uganda's Department of Meteorology in the Ministry of Water, Lands and Environment. The stations selected represented different geographical locations, the main sub-regions, various microclimates, and farming systems in Uganda. Due to the absence of weather stations, data for 12 virtual stations in Karamoja sub-region was downloaded from a NASA website[15]. The acquired datasets were used in CropWAT8 model[16] to compute GA's crop ET and effective rainfall and soil water balance. A series of 48 Moderate Resolution Imaging Spectroradiometers (MODIS) images for the East Africa region were downloaded from http://glovis.usgs.gov/. The images were for the period 2000 to 2011, each image represented a 10-day period of every month. Table 1 presents the characteristics of MODIS image.

**Table 1    MODIS image characteristics**

| Swath/km | Scene Size/km | Altitude/km | Revisit days |
|----------|--------------|-------------|--------------|
| 2330 | 10×10 | 705 | 16 |

The MODIS data were systematically converted into derived atmospheric, oceanic and the terrestrial products that were used in this study. The 500-meter resolution composites available from Global Visualization Viewer (GLOVIS) and Global Land Cover Facility (GLCF) were extracted from the MODIS level three surface reflectance products called MOD09A1. These monthly composites were necessary precursors to the MODIS Vegetation continuous fields' product. To understand relationship between Normalized Difference Vegetation Index (NDVI), Land Surface Temperature (LST) and Evaporative fraction or crop coefficient ($K_c$), two clear Land Sat Imagery (Table 2) for Karamoja sub-region for the dry months of January and February were obtained from GLOVIS (http://glovis.usgs.gov/). The study used a combination of meteorological data from ground stations and NASA's virtual synthetic data.

**Table 2    Characteristics of LandSat imagery used**

| Acquisition Date (yy/mm/dd) | Path | Row | Resolution/m |
|-----------------------------|------|-----|--------------|
| 2000-01-18 | 170 | 58 | 30×30 |
| 2001-02-05 | 170 | 59 | 30×30 |

## 2.3 Estimating evapotranspiration and effective rainfall from weather variables

Daily and monthly variables (minimum and maximum air temperature, Relative humidity, sunshine duration, wind speed, rainfall) were input to CropWAT (Version 8, 2009) to estimate reference evapotranspiration (PET) and effective rainfall (Pe). The PET was estimated using Penman-Monteith[17] which provided values that are consistent with actual crop use data worldwide. CropWAT8 estimated effective rainfall using the USDA SCS method at different stations using averaged rainfall data for the period 2000 to 2011. Crop coefficient ($K_c$) values of 0.45, 0.75, 1.15 and 0.75 for the initial (init), development (deve), mid-season (mid) and late season, respectively, were adopted to compute actual evapotranspiration of GA according to Mwangi[18]. For each station, total water requirement for GA was computed for a period of 90 d. In Karamoja sub-region, evapotranspiration was estimated using both the virtual station data sets and with SEBAL model using the methodology of Allen et al.[19]

The estimated values for GA's water requirement and irrigation requirement were allocated to each map unit within the area considered. The parameterized map surface was spatially interpolated[5,20] in ArcGIS v.9.3.1 to develop the continuous value illustration map for GA's water and irrigation requirement in Karamoja sub-region.

## 2.4 Estimating length of growing season and pattern

The length of the growing season for Karamoja sub-region was computed using NDVI time series. Sixteen-day MODIS composites for the period 2000 to 2011 were analyzed with the TIMESAT software (http://www.nateko.lu.se/personal/Lars.Eklundh/TIMESAT/login.asp) to compute crop phonological stages (emergence, heading (peak) and maturity (end of season). A ratio of average monthly rainfall ($P$) to average monthly potential reference evapotranspiration (PET) of 0.5[21] was used to draw distinction between periods of

water deficit and availability for crop production.

## 2.5    Estimation of the soil water balance in Karamoja sub-region

The soil water balance for Karamoja sub-region was evaluated by accounting for all ingoing and outgoing water in the root zone over a daily time step.    The water content was expressed as root zone depletion ($dr$) (Equation (1)).    The various parameters of soil water budget in equation are expressed in terms of water depth. The inputs in model for computation of soil water balance are indicated in Equation (1):

$$dr_i = dr_{i-1} + ETc_{adj} - P_i - I_i + (RO_i + DP_i) \qquad (1)$$

where, $dr$ is root zone depletion on days $i$ and $i-1$.    $dr$ is calculated prior to irrigation application, if any; $ETc_{adj}$ is Crop evapotranspiration under non-standard conditions on day $i$; $P$ is total rainfall over day $i$; $RO$ is water loss by runoff from the soil surface on day $i$; and $DP$ is water loss by deep percolation on day $i$.

## 2.6    Modeling the NDVI and retrieval of LST

Landsat Satellite images for Karamoja sub-region were used to estimate NDVI as a ratio of the reflectivities in Near Infrared (NIR referred to as band 4) and Infrared (IR referred to as band 3) regions of the electromagnetic spectrum.    Digital Numbers of NIR and IR bands were converted to Spectral radiance (Equation (2)):

$$L_\lambda = Gain \times DN + Bias \qquad (2)$$

where, $L_\lambda$ is radiance and $DN$ is digital number in imagery.

Gain and Bias were obtained from the header file. The latest gain and bias values for the Landsat 7 ETM+ sensor applied were comparable to those used elsewhere[22,23].    A raster calculator in ArcGIS v.9.3.1 (ESRI, Redlands, Cal.) was used to accomplish all computations and modeling.    A reduction in scene variability was achieved by converting the at sensor spectral radiance to exoatmospheric at Top of Atmosphere (TOA) reflectance (Equation (3)). Conversion to reflectance facilitated better comparison among the different scenes by removing difference caused by the position of the sun and the differing amounts of energy output by the sun in each band.

$$\rho_\lambda = \frac{\pi \times L_\lambda \times d^2}{E_{sun_\lambda} \times \cos\theta_s} \qquad (3)$$

where, $\rho_\lambda$ is planetary TOA reflectance; $\pi$ is mathematical constant; $L_\lambda$ is spectral radiance at sensor aperture; $d$ is Earth-Sun distance (astronomical units); $E_{sun\lambda}$ is mean exoatmospheric solar irradiance and $\theta$ is Solar Zenith angle.

During the conversion to reflectance, small negative values were created.    These values were not physical and were set to zero.    The NDVI was computed using the raster calculator (Equation (4)):

$$NDVI = \frac{\rho_4 - \rho_3}{\rho_4 + \rho_3} \qquad (4)$$

where, $\rho_4$ and $\rho_3$ is reflectivities for band 4 and band 3.

The effective at sensor brightness temperature ($T$) was determined using the Plank's inverse function in Equation (5)[24].    The spectral radiance, $L_\lambda$ was computed from Equation (2).    The calibration constants $K_1$ and $K_2$ were obtained from the Landsat data user's manual[25].

$$T = \frac{K_2}{\ln\left(1 + \dfrac{K_1}{L_\lambda}\right)} \qquad (5)$$

The final LST was estimated by Equation (6):

$$LST = \frac{T}{1 + \left(\lambda + \dfrac{T}{\rho}\right) \times \ln\varepsilon} \qquad (6)$$

where, $\lambda$ is wavelength of the emitted radiance which is equal to 11.5 $\mu$m; $\rho$ is $h\,c/\sigma$; $\sigma$ is Stefan Boltzmann's constant which is equal to $5.67 \times 10^{-8}$ Wm$^2$/K$^4$; $h$ is Plank's constant ($6.626 \times 10^{-34}$ J s); $c$ is velocity of light ($2.998 \times 10^8$ m/s); and $\varepsilon$ is spectral emissivity.

## 2.7    Modeling surface albedo in Karamoja sub-region

The changes in surface albedo and associated surface energy budget need to be understood[26] to improve the results image analysis.    The albedo at the top of atmosphere (atoa) referred to as albedo unadjusted, was determined according to Equation (7):

$$\alpha toa = \sum(\omega_\lambda \times \rho_\lambda) \qquad (7)$$

where, $\rho_\lambda$ is reflectivity and $\omega_\lambda$ is weighting coefficient for each band as indicated in Landsat 7 User's Handbook[27].    Values of the weighting coefficient were provided for each Landsat sensor in the appendix for handbook for Landsat images[27].    Surface albedo was corrected for atmospheric transmissivity) using Equation (8):

$$\alpha = \frac{\alpha toa - \alpha\,path - radiance}{\tau^2_{sw}} \qquad (8)$$

where, $\alpha\,path - radiance$ is to ranges between 0.025 to 0.04 and $\tau_{sw}$ is atmospheric transmissivity for direct solar beam radiation and diffuse radiation to the surface, calculated using Equation (9):

$$\tau_{sw} = 0.75 + 2 \times 10^{-5} z \qquad (9)$$

where, $z$ is roughness length.

## 2.8    Statistical analysis

Descriptive statistics (mean, standard deviation, minimum and maximum) were computed to understand the central tendency of the NDVI values. The coefficient of determination ($R^2$) were calculated and used to evaluate the adequacy of the fitted models between LST and NDVI, as well as between $K_c$ (crop coefficient) and NDVI.

## 3    Results and discussion

### 3.1    Length of the growing period and growing pattern

Two rainfall systems can be distinguished in Uganda, unimodal for semi-arid areas that stretch from South-Western to the North-East (Karamoja sub-region areas) and parts of West Nile (Arua). A bimodal pattern is observed for the rest of the country. To understand the growing pattern in Karamoja sub-region, a time series of NDVI was used to identify physiological stages of vegetation growth. The NDVI values computed for Karamoja sub-region ranged between −1 to +1, values close to +1 indicated high vegetation vigor while values close to zero indicate low vegetation vigor. Negative indicated water bodies especially in south eastern end of the region with vast number of wetland lands. The Minimum NDVI value was about 0.3 in February and a maximum of about 0.68 in July (Figure 2). In Figure 2, increase in NDVI towards from mid-February indicates Greening up while decline in NDVI values after July corresponds to greening down. The greening up indicates the start of the growing period and greening down implied maturity thus end of the growing period for the sub-region. The NDVI Peak values in the month of July imply laxity of rainfall. This correlates well with unimodal rainfall regime of Karamoja sub-region[28] that commences from April to November with rainfall peaks

during April, May, July and August with laxity of rains during the month of June. The unimodal rainfall regime is supplied with moisture from the Congo basin[29,30]. These results were in agreement with farming activities in Karamoja sub-region which begin with land preparation during the lean season starting towards end of February. Crop establishment occurs during the rainy season from April to October and main harvest from August to December.
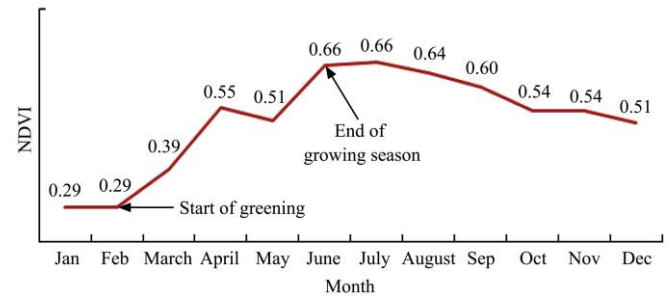
Figure 2    Temporal variation of NDVI in Karamoja sub-region

Figure 3 presents the spatial distribution of NDVI during July, September, October, November and December for the Karamoja sub-region processed from the MODIS images. The images indicate spatial and temporal variability of NDVI in Karamoja sub-region. The central part of Karamoja region (Kotido, Moroto and Napak) consistently had the least NDVI values during these months. NDVI values higher than 0.73 were determined in July for the western areas of the sub-region, while eastern areas had NDVI values higher than 0.68 during November and December. During the wet season the sub-region's average NDVI values was 0.46±0.05, while NDVI values in dry season had a range of 0.41±0.05. The variation of NDVI values is consistent with the spatial and temporal variation of the rain season in the sub-region. With regards to land cover, woodland areas had an average NDVI of 0.53±0.05, grasslands of 0.49±0.07, thickets and shrub lands of 0.40±0.04, croplands/croplands of 0.30±0.00 and bush lands of 0.52±0.05. There was a slight variation at land cover type level with a major variation due to seasonal variations.

The critical ratio, Pe/PET exceeds 0.50 for Arua, Entebbe, Namulonge, Jinja, Gulu, Kabale and Kampala, from March to December expect Kasese (Figure 4), where Pe/PET was less than 0.50 for most parts of the year. Arua, Namulonge, Jinja, Gulu, Kabale and Kampala

had Pe/PET of 1.03, 1.01, 1.16, 1.00, 0.90 and 1.13, respectively. Critical ratios less than unity indicated that the effective rainfall (Pe) was less than potential evapotranspiration and vice versa for critical ratios greater than unity. A ratio 0.40 indicated arid climate while semi-arid climate is represented by a range of 0.40 to 0.80. The length of growing period for semi-arid areas ranged between 60 to 119 days.
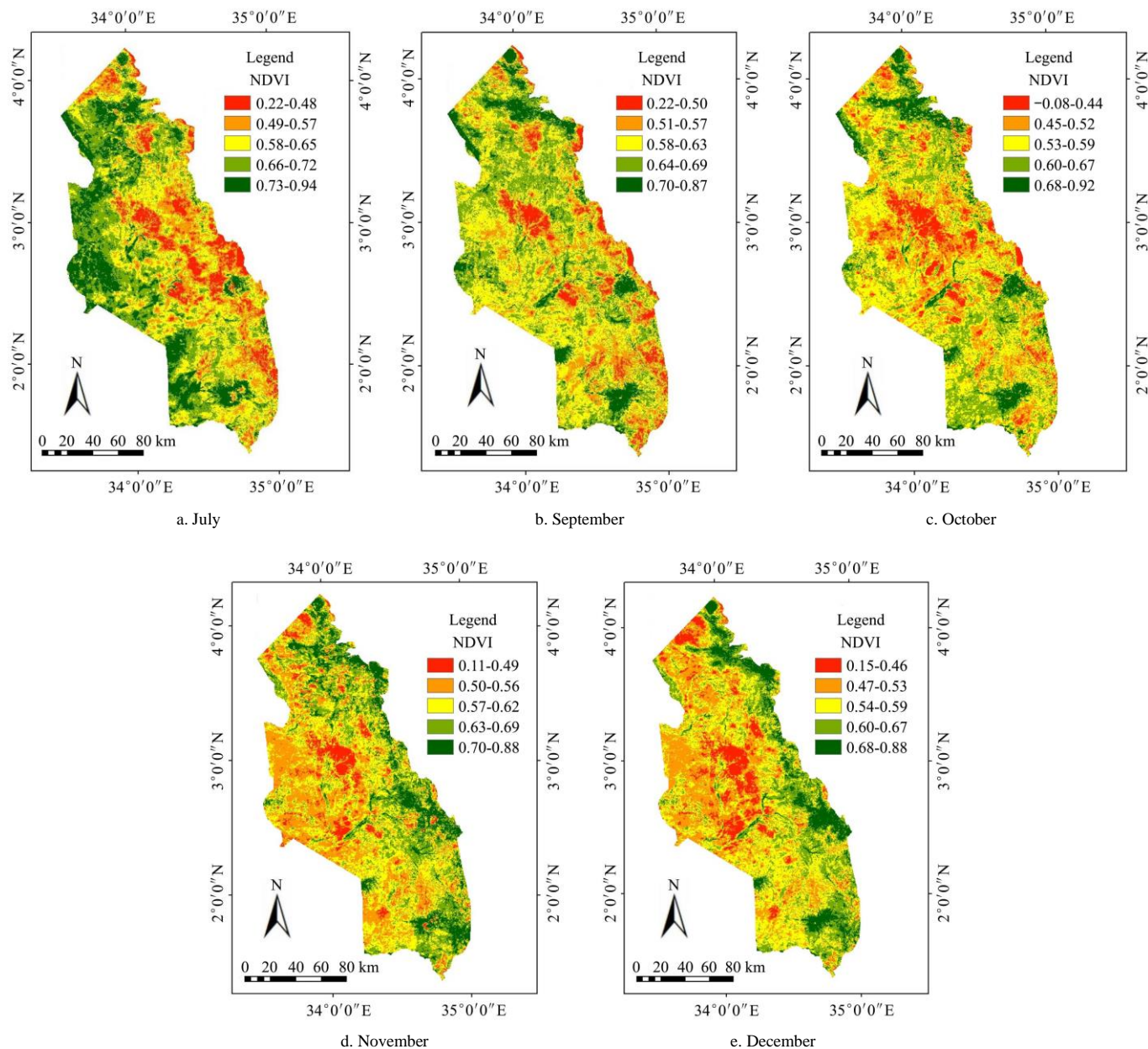
Figure 3    Spatial distribution of NDVI based on MODIS images for July, September, October, November and December

Critical ratios from 0.80 to 1.20 correspond to sub-humid (growing period 180-269 days) and those greater than 1.20 correspond to humid (growing period greater than 270 days); Kasese and Mbarara had averages 0.42 and 0.83, respectively, which was an indication of the semiarid climate, this was also reported by Mubiru[3]. Only Entebbe was found to be humid with Pe/PET ratio of 1.47 while the rest of the stations had a sub-humid climate. The growing period in Entebbe, Namulonge, Jinja, Gulu, Kabale and Kampala extended from end of February to late June while second growing season started from August to December. Two planting seasons are possible in Masindi, Jinja, Mbarara, Tororo, Soroti, Gulu, Lira, Namulonge, Entebbe, Kampala and Kabale. The growing season in Arua and Karamoja sub-region was observed to start in early March to late September (Figure 4).
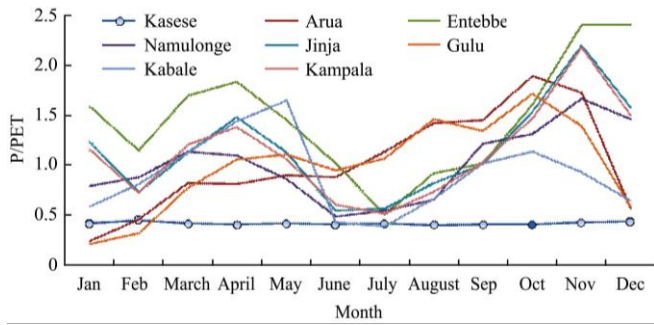
Figure 4    Variation of P/PET for various locations throughout the year

## 3.2    Assessment of soil water balance in Karamoja sub-region

The initial moisture depletion at the start of the dry season in the late September was expressed as a percentage of the Total Available Moisture (TAM). Naturally the soil water reserves are due to the previous rains (Figure 5).    The dominant soils were black clays and dark grey with low organic matter and low to medium moisture storage capacity.    These soils may be productive when irrigated; however, soil water balance indicated that they experience high water deficits towards the end of the growing season (Figure 6).    The soil water balance in Karamoja sub-region is mostly positive for the period of 15-20 d after planting and thereafter experiences an increasing deficit of 60 mm to 80 mm (Figure 5).    The irregular rains May to mid-July replenish the reserves (Figure 6).    The period of heavy rains between July to late November is characterized by frequent rains that exceed the evaporative demand. However after November the crop water requirement exceed the effective rainfall.    The soil water balance analysis indicated that if GA is planted in late September, the soil moisture in the root zone is sufficient for initial vegetative growth.    This is a requirement to ensure that GA will survive the following elongated drought period in order to eliminate the break in food production cycle of Karamoja sub-region.
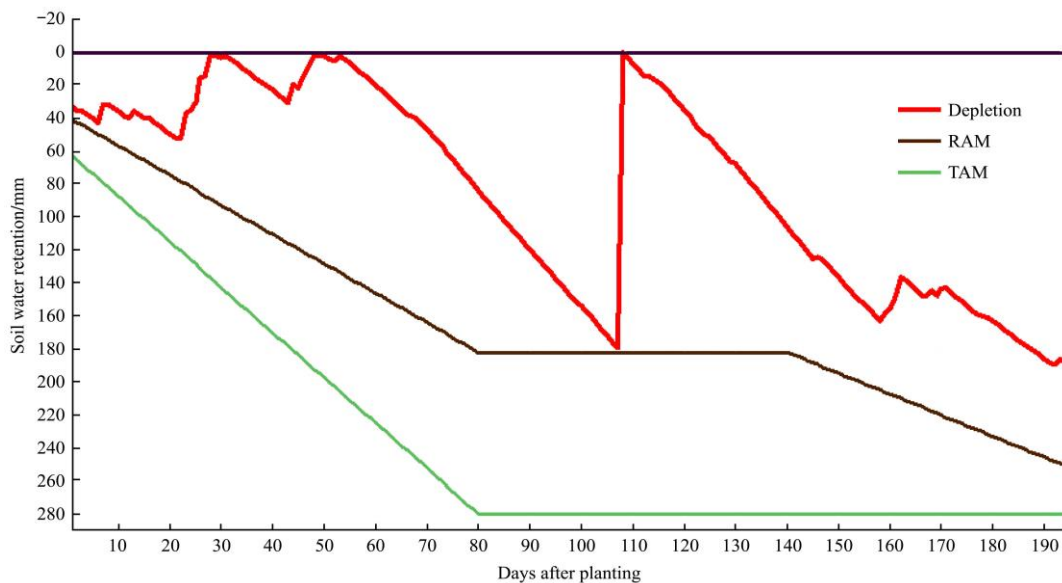


Figure 5    Soil water balance based on the depletion rate, available soil moisture and total soil moisture
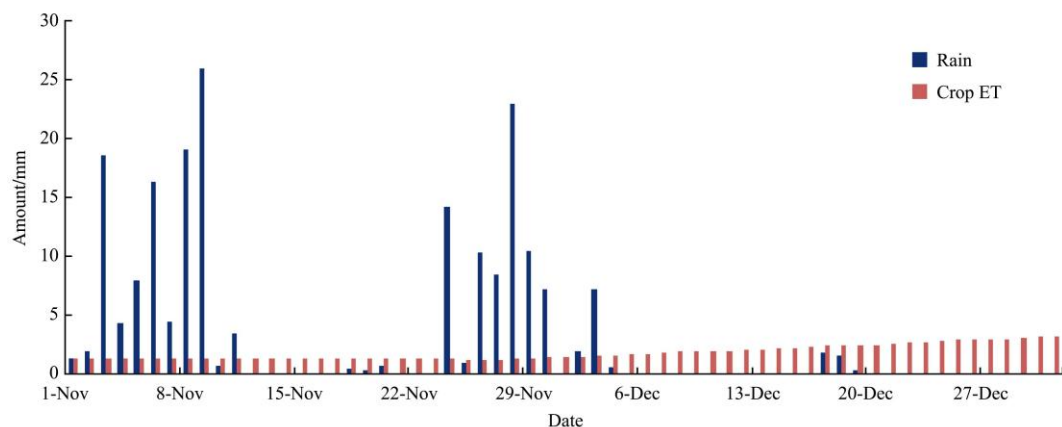


Figure 6    Effective rain and actual evapotranspiration for grain Amaranth in Karamoja sub-region

## 3.3    Estimation of LST from Landsat imagery

The highest land surface temperatures existed for the bare soils or areas with sparse vegetation.    A number of random samples from the LST images (Table 3) and NDVI images indicated that the LST was lower with increased vegetation cover.    This is expected as the vegetation canopy intercepts the incoming solar radiation[1,31].    Higher land surface temperatures increase plant weight and leaf area but the Leaf Area Ratio (LAR) is reduced[32].    A negative correlation between the LST and NDVI was observed with $R^2$ value of 0.65 (Figure 7). Solar radiation is the predominant factor driving the correlation between LST and NDVI[33] during the beginning and at the end of the growing season. Positive correlation between LST and NDVI existed for highland areas.    According to Karnieli et al.[33], positive correlation is possible when energy is the limiting factor for vegetation growth like in higher altitudes and latitudes. Mid-season the radiative flux might not have been high enough to limit vegetation growth and solar radiation played a smaller role in determining the nature of the LST to NDVI correlation.    Partial variability of LST showed a thermal gradient from the densely vegetated areas around Mountain Elgon to drier areas of Nakapiripirit and Moroto further to areas of Kotido as well as areas altered by urban establishments.    It was observed that radiative properties and thermal properties; moisture content values affect the determined LST.    The urban areas exhibited the highest temperatures, followed by the bare soils. The surface temperatures in Karamoja sub-region were similarly documented to be high. Generally, land surface temperatures are higher in the dry period with vegetation conditions deteriorating faster in the dry period of January to February.

### Table 3    Mean LST for different images

| Image Path/Row | Acquisition Date | Mean LST | Standard deviation |
|---|---|---|---|
| P170r058 | 18/01/2000 | 35.85 | 3.86 |
| P170/R059 | 05/02/2001 | 29.50 | 5.39 |

The higher biomass land cover had lower land surface temperatures except for urban development land use where a lot of materials exit with different reflectivity signatures.    However, the extent of urban development is rather low in Karamoja sub-region and thus restricts areas where the negative correlation exists.    The NDVI accounted for 65% of variability in LST (Figure 7). However, caution needs to be taken since a large $R^2$ does not imply the regression model will provide accurate predictions in the future since it can easily be inflated if variables are related in a nonlinear fashion.    The negative NDVI values were attributed to the combined effect of different land uses, bare rocks, urban centers and stony mountains with no or little vegetation. Similar trends were also observed by Rafn et al.[34]    These reflect in different bands of electromagnetic spectrum other than visible and near infrared region.    In addition, the NDVI was developed to be sensitive to green vegetation[6]. NDVI is a good predictor of vegetation vigor over grasslands which are dominant in Karamoja sub-region though the spectral differences between different plant stages has to be taken into account[35].
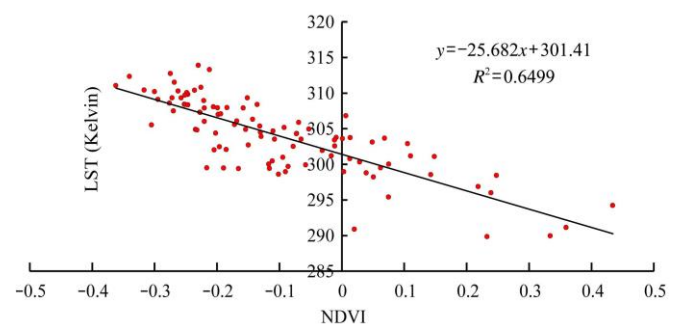


Figure 7    LST against NDVI plot

## 3.4    Evapotranspiration estimation with SEBAL model from Landsat imagery

In Figure 8, the correlations between $K_c$ and NDVI extracted from Land sat images indicated negative $K_c$ values derived by the SEBAL model from satellite imagery which have no physical meaning[34].    The NDVI which is a normalized index based on ratios of spectral band intensities do occasionally take on negative value, this can produce negative $K_c$ values.    The positive $K_c$ values represent fraction climatic demand of the atmosphere that is actually used to evaporate and transpire water.    According to the SEBAL model the $K_c$ value was equivalent to the evaporative fraction.    The $K_c$ possessed distinct spatial character and was influenced by crop type, soil evaporation, climatic conditions, crop growth stages and land uses based on 30 m by 30 m pixel basis.
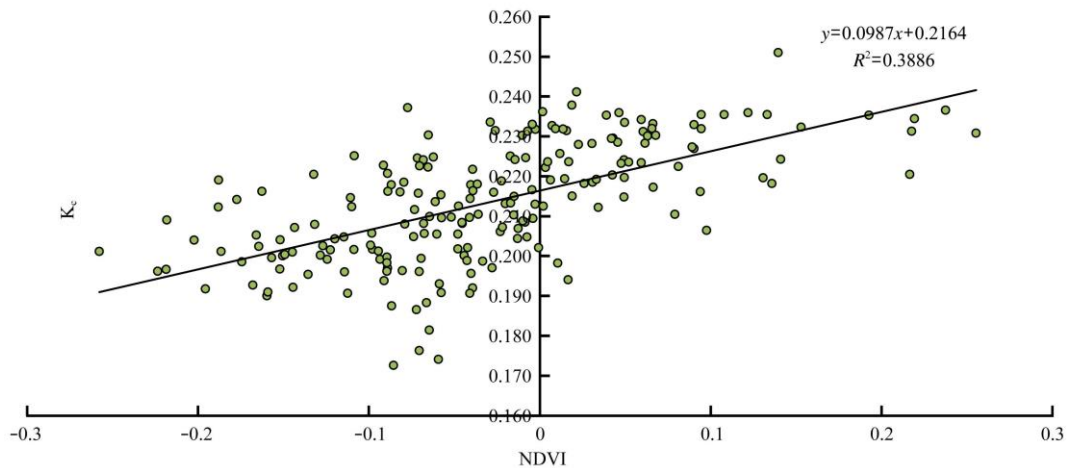
Figure 8    Correlations between $K_c$ and NDVI extracted from Land sat images

The daily ET by SEBAL model ranged from 3.24 mm to 4.78 mm based on the land use/cover. Comparison of SEBAL model with CropWAT8 model revealed that Karamoja sub-region highest values of ET and crop water demand. SEBAL model could not be effectively applied to compute latent heat fluxes in areas of low vegetation, highland areas and arid environments like Karamoja sub-region though it can be used to represent the spatial distribution of latent heat fluxes. This was primarily due to an inability of SEBAL model to adequately represent the Bowen ratio under such conditions. Sensible heat loss and evaporative heat loss are the most important processes in the regulation of leaf temperature[36]. When evaporation rate is low, water supply is limited and the Bowen ratio tends to be high[37]. The poor partitioning of the Bowen ratio was partly due to low latent heat fluxes at the wettest pixels; SEBAL was left with a very small sensible heat flux gradient between the cold and hot pixels.

## 3.5    Surface albedo in Karamoja sub-region in relation to soil suitability

Surface albedo Values from the SEBAL model ranged from 0.025-0.500. Areas of Kotido, Moroto had values of 0.25 to 0.50 while southern areas of Nakapiripiti and Amudat towards hilly areas of Kapachorwa to mountain Elgon had albedo values in the range of 0.1 to 0.2 (Figure 1). The soils in the southern part of sub-region appeared to be dark colored with high moisture content due to lower surface albedo values. The nature of soil surface was derived from surface albedo values which ranged from 0.03 to 0.30 for low

values and 0.4 to 0.5 for high values of indicating short grasslands, meadows and shrub lands[38]. Surface albedo images show that the soils are of rough dark color surfaces to smooth light colored soil surfaces. The areas which had a low surface albedo, low surface temperature, high vegetation index area were bound to have high evapotranspiration levels. The converse was true for areas with low vegetation indices; these had high surface albedo, high surface temperatures and thus low evapotranspiration. Table 4 indicates cropland, grassland and dark colored surfaces dominant in the study areas. Lower surface albedo was observed in areas around Lake Kyoga and mountain Elgon with higher surface albedo values towards the Karamoja sub region. Organic matter was another possible soil coloring agent. High soil organic matter increased the absorbance of the soils thus resulting in lower albedo values. The higher organic content level was an indication of higher suitability for crop production. The distribution of surface albedo is important for planning of irrigation scheduling and estimation of water resources in agricultural areas[39]. Knowledge of the temporal and spatial distribution of the surface albedo is important in the investigation of earth climate and its variability at multiple times scales[40]. The areas which had a low surface albedo, low surface temperature, high vegetation index area were bound to have high evapotranspiration levels. The converse was true for areas with low vegetation indices; these had high surface albedo, high surface temperatures and thus low evapotranspiration.

**Table 4    Mean and standard deviation for surface albedo for areas of Eastern and North Eastern Uganda**

| Image | Acquisition date | Mean | Standard deviation |
|-------|------------------|------|--------------------|
| 170/58 | 2000-01-18 | 0.13 | 0.04 |
| 170/59 | 2001-02-05 | 0.15 | 0.04 |

## 3.6    NDVI in relation to GA suitability

The NDVI values for most of the Karamoja region were negative and just slightly greater than 0 with mean values close to zero.    Positive values near zero indicate bare soils and higher positive values of NDVI ranging from sparse vegetation 0.1-0.5 to 0.6 for dense green vegetation (Table 5).    Low vegetation indices were due to the existences of large expanses of bare soil.    The bare soil and soil background effect influenced the reflected radiance of the actual values by about 20% thus very low NDVI values.    Vegetation canopies in semi-arid areas like Karamoja is mainly thickets and shrubs, grasslands which do not achieve complete coverage making the NDVI susceptible to the spectral influence of the soil and soil moisture in gaps between vegetation[41,42].    The negative and low NDVI values are an indication of drought conditions.    The NDVI gave the extent of water status.    The low NDVI values indicted water stress leading to wilting and yellowing due to prolonged dry spells.

**Table 5    Statistical analysis of NDVI maps from Landsatimages**

| Images path/row | Acquisition date | Minimum NDVI | Mean NDVI | Maximum NDVI | Standard deviation |
|-----------------|------------------|--------------|-----------|--------------|--------------------|
| P170r058 | 18/01/2000 | -0.21 | -0.06 | 0.35 | 0.08 |
| P170/R059 | 05/02/2001 | -0.34 | -0.107 | 0.30 | 0.17 |

## 3.7    Grain Amaranth water requirements

The highest average reference evapotranspiration of 4.27 mm/d was observes in June for Kasese while Kabale had the lowest value of 1.61 mm/d.    Kasese had the highest annual average ET of 3.28 mm/d while Entebbe had the lowest annual average of 2.38 mm/d.    Based on results from CROPWAT model, Tororo had the lowest crop water demand of 174.1 mm/season while Lira had the highest of 267.4 mm/season (Table 6).    Crops are expected to have highest water demands during months of May, June to August for all stations except for Kabale and Mbarara where the highest water demands are expected between November and February.    Kasese

results are presented due to its semi-arid climate.    GA growing in Kasese requires 206.2 mm of water if planted in mid-September with a water deficit of 1.4 mm. Comparison of actual ET for GA with effective rainfall at most station shows no or minor water deficits at all stations.    In Mbarara a semi-arid area, GA planted on the early March experienced a water deficit of 3.2 mm. However the crops have be planted at an appropriate time of the year to benefit from the soil moisture from rains for emergence of the seedling and initial vegetative growth. Using the 12 virtual stations in Karamoja sub-region CROPWAT8 model showed that the GA water demands ranged between 467.5 mm (Figure 9) for areas of central to eastern Karamoja (Kotido and Moroto) to 447.1 mm in southern part of region (in Nakipiripiriti and Amudat). FAO[21] approximated water demands for seasonal annual crops like maize and cotton to be between 500-800 mm and 700-1300 mm respectively which values are far much higher than the GA water demands in same sub-region. Karamoja sub-region had the highest water demands for GA which was attributed to high wind speeds, higher temperatures and low relative humidity.    The high atmospheric demand drives crop water demands higher. The highest GA water demands exist in the drier areas of Kotido (Central of Karamoja region), Moroto (East of Karamoja region) and Kaabong (Northeastern of Karamoja).    Karamoja sub-region had the shortest growing season in Uganda yet most crop production is mainly rainfed.

**Table 6    GA water requirements at different stations in Uganda**

| Location | Planting date | Harvest date | Etc /mm | Effective Rainfall/mm | Irrigation requirement/mm |
|----------|---------------|--------------|---------|-----------------------|---------------------------|
| Tororo | 12/10/2012 | 10/01/2013 | 174.1 | 293.8 | 1.8 |
| Malinda | 11/09/2012 | 10/12/2012 | 185.3 | 303.7 | 0.0 |
| Kabale | 23/02/2012 | 24/05/2012 | 189.4 | 280.3 | 0.0 |
| Mbarara | 07/03/2012 | 05/06/2012 | 193.8 | 246.0 | 3.2 |
| Kasese | 14/09/2012 | 13/12/2012 | 203.1 | 288.1 | 0.0 |
| Entebbe | 01/03/2012 | 30/05/2012 | 213.7 | 398.9 | 0.0 |
| Arua | 11/03/2012 | 09/11/2012 | 217.7 | 396.6 | 0.0 |
| Namulonge | 11/08//2012 | 09/11/2012 | 243.1 | 294.0 | 0.0 |
| soroti | 02/08/2012 | 31/10/2012 | 244.8 | 347.4 | 0.0 |
| Kampala | 26/02/2012 | 27/05/2012 | 245.2 | 317.9 | 0.0 |
| Jinja | 02/03/2012 | 31/05/2012 | 263.2 | 343.2 | 0.0 |
| Gulu | 12/07/2012 | 10/10/2012 | 264.1 | 382.4 | 0.0 |
| Lira | 12/08/2012 | 10/11/2012 | 267.4 | 385.3 | 0.0 |
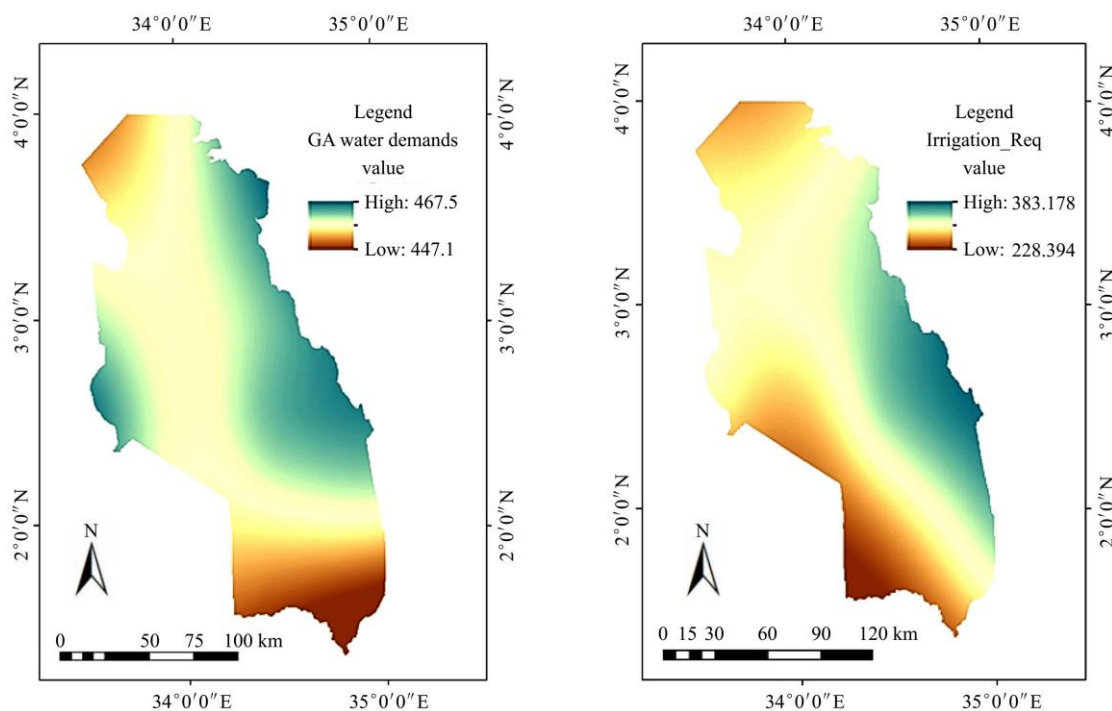
Figure 9    GA water demand and irrigation requirement for Karamoja sub-region

## 6    Conclusions

The research demonstrated that openly available meteorological data can be applied in the determination crop water requirement in areas with a low density of operational ground meteorological stations as is the case in Uganda.    Nonetheless there were variations, with the results of the simulative weather data do not equal the actual, and thus, some extent errors in light of SEBAL model calculation.    The accurate estimation of ET especially in semi-arid areas like Karamoja greatly relies by the spatial resolution of virtual stations and ability of user to refine the satellite imagery to cater for soil back scattering effect especially for bare grounds and also apply SEBAL model for different seasons.    The SEBAL model underestimates key parameters especially in arid and semi-arid areas.    With regards to crop water requirements, the available moisture after the end of the rainy season in the most drought severe region of Karamoja sub-region would propel the GA to maturity. This would potentially contribute to continuity of the food production cycle in Karamoja sub-region.    Given the water requirement of GA, it could be successfully grown in all regions of Uganda.    The potential to grow GA in various parts of the country was attributed to the short maturity period of the crop and its drought resilience.    The combination of using GIS and SEBAL model were effective tools in determining suitable GA growing periods in different parts of Uganda.

## Acknowledgement

## [References]

[1]    Kabenge I, Irmak S, Meyer G E, Gilley J E, Knezevic S, Arkebauer T J, et al.    Evapotranspiration and surface energy balance of a common reed-dominated riparian system in the Platte River Basin, Central Nebraska.    Trans. ASABE, 2013; 56: 135–153.

[2]    Musiitwa F, Komutunga E T.    Agricultural systems.    In: Agriculture in Uganda.    Fountain Publishers, Kampala, Uganda. 2001.

[3]    Mubiru D N.    Climate change and adaptation options in Karamoja.    A report submitted to FAO and EU. 2010. http://www.disasterriskreduction.net.    Available online [2015-01-07]

[4]    Muyonga J H, Ugen M, Bisikwa J, Nakimbugwe D, Masinde D, Bbemba J, et al.    Promoting production and utilization of grain amaranth for improved nutrition and health in Uganda. Annual progress report, submitted to McKnight Foundation. 2010.

[5]   Mulder V L de Bruin S, Schaepman M E, Mayr T R.   The use of remote sensing in soil and terrain mapping. Geoderma, 2011; 162: 1–19.

[6]   Qi J, Marsett R, Heilman P, Biedenbender S, Moran M S, Goodrich D.   RANGES improves satellite-based information and land cover assessments in southwest United States.   EOS, Trans. Am. Geophys. Union, 2002; 83(51): 601, 605−606.

[7]   Bastiaanssen W G M.   SEBAL-based sensible and latent heat fluxes in the irrigated Gedi Basin Turkey.   J. Hydrol., 2000; 229 (1-2): 87−100.

[8]   Bastiaanssen W G M, Menenti M, Feddes R A, Holtslag A A M.   A remote sensing surface energy balance algorithm for land (SEBAL).   1. Formulation. J. Hydrol, 1998; 198–212.

[9]   Allen R G, Morse A, Tasumi M, Trezza R, Bastiaanssen W G M, et al.   Evapotranspiration from a satellite based surface Energy Balance for the Snake Plain Aquifer in Idaho Proc. USID Conf. San Luis Obispo, CA, USA, July 2002.

[10]  Farah H O, Bastiaanssen W G M.   Spatial variations of surface parameters and related evaporation in the lake Naivasha Basin estimated from remote sensing measurements. J. Hydrol., 2001; 15: 1585-1607.

[11]  Bastiaanssen W G M, Chandrapala L, Water balance variability across Sri Lanka for assessing agricultural and environmental water use.   J. Agric. Wat. Manage, 2003; 58: 171–192.

[12]  Bastiaanssen W G M, Ahmad M D, Chemin Y.   Satellite surveillance of evaporative depletion across the Indus Basin. Water Resource Res, 2002; 38(12): 1–9.

[13]  Bastiaanssen W G M, Noordman E J M, Pelgrum H, Davids G, Thoreson B P, Allen R G.   SEBAL model with remotely sensed data to improve water resource management under actual field conditions.   J. Irrig. Drain. Eng., 2005; 131(1): 85-93.

[14]  UBOS.   2013.   Statistical abstracts. http://www.ubos.org/ onlinefiles/uploads/ubos/pdf%20documents/abstracts/Statisti cal%20Abstract%202013.pdf. Available online [2014-02-27]

[15]  NASA.   2014.   http://power.larc.nasa.gov/cgibin/cgiwrap/ solar/agro.cgi?email=agroclim@larc.nasa.gov.   Available online [2014-02-02]

[16]  Clarke D, Smith M, Askari K E.   CROPWAT for windows: user guide.   Food and Agriculture Organization of the United Nations, 1998.

[17]  Allen R G, Pereira L S, Raes D, Smith M.   Crop evapotranspiration: guidelines for computing crop water requirements.   Irrig. Drain. Pap. No. 56. FAO, Rome, Italy. 1998.

[18]  Mwangi D, Introduction to Grain Amaranth.   Joy pet Services and Printers Ltd., Nairobi, Kenya. 2003.

[19]  Allen R G, Tasumi M, Trezza R.   SEBAL (surface energy

balance algorithms for land).advanced training and users manual.   Idaho Implementation (version 1.0). 2002.

[20]  Hong S Y, Minasny B, Han K H, Kim Y, Lee K.   Predicting and mapping soil available water capacity in Korea.   Peer J.1, 2013; 71.

[21]  FAO.   1996.   Agro-ecological zoning guidelines.   FAO Soils Bulletin 73.

[22]  Chander G, Markham B L, Helder D L.   Summary of current radiometric calibration coefficients for Landsat MSS, TM, ETM+, and EO-1 ALI sensors.   Rem. Sens. Env., 2009; 113(5): 893−903.

[23]  Goslee S C.   Analyzing remote sensing data in R: the landsat package.   J. Stat. Soft. 2011; 43(4): 1−25.

[24]  Rajeshwari A, Mani N D.   Estimation of land surface temperature of Dindigul district using Landsat 8 data.   Int. J. Res. Eng. Tech., 2014; 2321−7303.

[25]  Landsat Project Science Office, 2002.Landsat 7 Science Data User's Handbook.Goddard Space Flight Center, Greenbelt, MD.

[26]  Forster P, Ramaswamy V, Artaxo P, Berntsen T, Betts R, Fahey D W, et al.   Changes in atmospheric constituents and in radiative forcing, in: climate change: the physical science basis.   Contribution of working group i to the fourth assessment report of the intergovernmental panel on climate change, Cambridge University Press, Cambridge, United Kingdom and New York, NY, USA, 2007.

[27]  NASA, 2013.   The Landsat 7 science data user's handbook. http://landsathandbook.gsfc.nasa.gov/. Available online [2014-02-01]

[28]  Owiti Z, Zhu W.   Spatial distribution of rainfall seasonality over East Africa.   J. Geog. Reg. Plan., 2012; 5(15): 409−421.

[29]  Phillips J, McIntyre B.   ENSO and interannual rainfall variability in Uganda: Implications for agricultural management.   Int. J. Climatol., 2000; 20:171–182.

[30]  Mubiru D N, Komutunga E, Agona A, Apok A, Ngara T. Characterising agrometeorological climate risks and uncertainties: Crop production in Uganda.   S. Afr. J. Sci., 2012; 108(3-4):108–118.

[31]  Lafleur P M.   Connecting atmosphere and wetland: Energy and water vapor exchange.   Geography Compass, 2008; 2(4): 1027–1057.

[32]  Milla R N, Reich P B.   Multi-trait interactions, not phylogeny, fine-tune leaf size reduction with increasing altitude.   Annals of Botany, 2011; pp.1−11.

[33]  Karnieli A, Nurit A, Rachel T, Pinker Martha A, Marc L, Imhoff Garik G, et al.   Use of NDVI and land surface temperature for drought assessment: merits and limitations. J. Clim., 2010; 23: 618–633.

[34]  Rafn E B, Contor B, Ames DP.   Evaluation of a method for estimating irrigated crop transpiration coefficients from

remotely SensedData in Idaho.  J.Irrig. Drain.Eng., 2008; 134(6): 722.

[35] Kondoh A, Higuchi A.    Relationship between satellite-derived spectral brightness and evapotranspiration from grassland.  J. Hydrol. Proc., 2001; 15: 1761−1770.

[36] Bowen I S.  The ratio of heat losses by conduction and by evaporation from any water surface.  Physical Rev., 1926; 27: 779−787.

[37] Nobel P S.  Physiochemical and environmental plant physiology.  4th ed. Academic Press, San Diego, CA, USA. 1999.

[38] Salifu T, Agyare W A.  Distinguishing different land use types using surface albedo and normalized difference vegetation index derived from the SEBAL for the Atankwidi and a farm sub catchments in Ghana.  J. Eng. Appl. Sci.,

2012; 7(1): 69−80.

[39] Tani H.  Estimation of surface albedo from NOAAAVHRR data.  J. Fac. Agric., Hokkaido University., 1992; 65(4): 331−341.

[40] Allen R G, Tasumi M, Trezza R.  METRICT: Mapping evapotranspiration at high resolution.  Applications Manual for Landsat Satellite Imagery. Version 2.0.3, University of Idaho, Kimberly, Idaho, USA. 2007.

[41] Kremer R G, Running S W.  Community type differentiation using NOAA/AVHRR data within a sagebrush-steppe ecosystem.  Rem. Sens. Environ., 1993; 46: 311–318.

[42] Peters A J, Eve M D.  Satellite monitoring of desert plant community response to moisture availability.  Environ. Monit. Assess, 1995; 37: 273–287.